# Solitonization of a dispersive wave

F. Braud, M. Conforti, A. Cassez, A. Mussot, A Kudlinski

# Solitonization of a dispersive wave

F. Braud, M. Conforti, A. Cassez, A. Mussot, A Kudlinski

# Solitonization of a dispersive wave

F. BRAUD[1], M. CONFORTI[1], A. CASSEZ[1], A. MUSSOT[1], AND A. KUDLINSKI[*]

[1] Univ. Lille, CNRS, UMR 8523 - PhLAM - Physique des Lasers Atomes et Molécules, F-59000 Lille, France
[*] Corresponding author: alexandre.kudlinski@univ-lille1.fr

Compiled March 2, 2016

**We report the observation of a nonlinear propagation scenario in which a dispersive wave is transformed into a fundamental soliton in an axially-varying optical fiber. The dispersive wave is initially emitted in normal dispersion region and the fiber properties change longitudinally so that the dispersion becomes anomalous at the dispersive wave wavelength, which allows it to be transformed into a soliton. The solitonic na-ture of the field is demonstrated by solving the di-rect Zakharov-Shabat scattering problem. Experimen-tal characterization performed in spectral and temporal domains show evidence of the solitonizatin process in an axially-varying photonic crystal fiber.**

***OCIS codes:*** *(190.4370) Nonlinear optics, fibers; (190.5530) Pulse propagation and temporal solitons.*

http://dx.doi.org/10.1364/ao.XX.XXXXXX

Since their first observation in optical fibers four decades ago [1], temporal solitons have been the subject of intense research both from the fundamental and application point of views [2]. Initially thought to revolutionize long-haul high-speed telecommunications [3], their field of applications has progressively moved towards the development of all-fiber ultrashort sources using cavity or single-pass configurations [2]. Indeed, the intrinsic Fourier-transform limited nature of fundamental solitons and the fact that they are very robust against perturbations, make them very attractive for a number of applications such as nonlinear microscopy and endoscopy [4–6].

Fundamental solitons can be excited in anomalous dispersion optical fibers using ultrashort pulses matching as closely as possible the $N = 1$ condition, $N$ being the soliton order [7]. When the input pulse is not close enough to this condi-tion, a higher-order soliton (corresponding to $N > 1$) can be excited, which breaks up into $n$ fundamental solitons through the fission mechanism [8–10], where $n$ is the closest integer to $N$. Depending on fiber properties and input pulse parameters, the generation of a soliton can be accompanied by the emission of a resonant radiation, in the form of a dispersive wave [11]. In particular, this occurs when the soliton is close enough to the fiber zero dispersion wavelength (ZDW) so that its spectrum overlaps with the normal dispersion region [12, 13]. This highly dispersive radiation usually has a very low peak power so that it does not experience any nonlinear effect, unless axially-varying fibers are employed to alter its dynamics [14]. In this case, it has been shown that longitudinally adjusting the fiber dispersion can help keeping the dispersive wave powerful enough to initiate a nonlinear cascading process.

In this work we show numerically and experimentally that a dispersive wave initially emitted from a soliton can be transformed itself into a fundamental soliton, a process that we termed solitonization. This is achieved by using an axially-varying fiber where the longitudinal evolution of dispersion is tailored to compress the initially dispersive wave into a femtosecond-scale pulse. The solitonic nature of this pulse is demonstrated by solving the direct Zakharov-Shabat (ZS) scattering problem, giving results that are in good agreement with simulations and experimental measurements. The term solitonization has been already used in the field of Anderson localization, to denote the nonlinear modification to the localized state induced by a (linear) disordered potential [15]. The process under study here is quite different, since no linearly localized states exist in the fiber.

Let us start the study with numerical simulations based on the following generalized nonlinear Schrödinger equation (GNLSE):

$$i\partial_z A + D(i\partial_t, z)A + \gamma(z)\left(A\int R(t')|A(t-t')|^2\right) = 0, \quad \textbf{(1)}$$

where $D(i\partial_t, z) = \sum_{n\geq 2} \frac{\beta_n(z)}{n!}(i\partial_t)^n$ is the dispersion operator, which takes into account the full dispersion profile of the fiber, $\gamma$ is the nonlinear coefficient, $R(t) = (1 - f_R)\delta(t) + f_R h_R(t)$ includes both instantaneous (Kerr) and Raman response ($f_R = 0.18$) [16], $\omega_p$ is the pump carrier frequency, around which $D(i\partial_t)$ is expanded, and $t$ is the retarded time in the frame traveling at natural group velocity $V_g = V_g(\omega_p) = \beta_1^{-1}$. We neglected the frequency dependence of the nonlinear coefficient and the self-steepening term, because we verified that they do not play any significant role for the pulse durations we are using. The fiber under investigation is a photonic crystal fiber (PCF), with values of the pitch ($\Lambda$) and normalized hole diameter ($d/\Lambda$, $d$ being the hole diameter) respectively equal to 2.06 $\mu$m and 0.62. The PCF parameters were calculated using the model from [17]. The value of dispersion and nonlinear parameter are respectively $\beta_2 = -8 \times 10^{-28}$ s$^2$/m and $\gamma = 0.042$ (W.m)$^{-1}$ at the pump wavelength of 881 nm. The fiber was designed to excite a fundamental soliton using pulses from a standard Ti:Sa oscillator delivering Gaussian Fourier transform limited pulses of 140 fs full width at half maximum (FWHM) du-

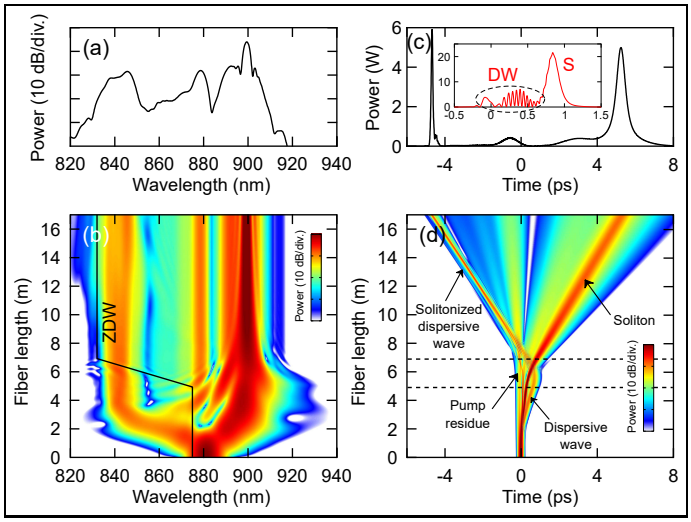


**Fig. 1.** Numerical simulations showing solitonization of a dispersive wave. (a) Output spectrum and (c) temporal trace after 17 m of propagation. The inset in (c) corresponds to the temporal trace at a fiber length of 7 m, i.e. just after the dispersive wave has crossed the ZDW and has entered the anomalous dispersion region. The dispersive wave (DW) that will be solitonized is surrounded by the dashed black line, and S is the soliton. (b) Spectral and (d) temporal dynamics with fiber length. The black line in (b) is the ZDW. Black dashed lines in (d) depict the start and end of the tapered section.

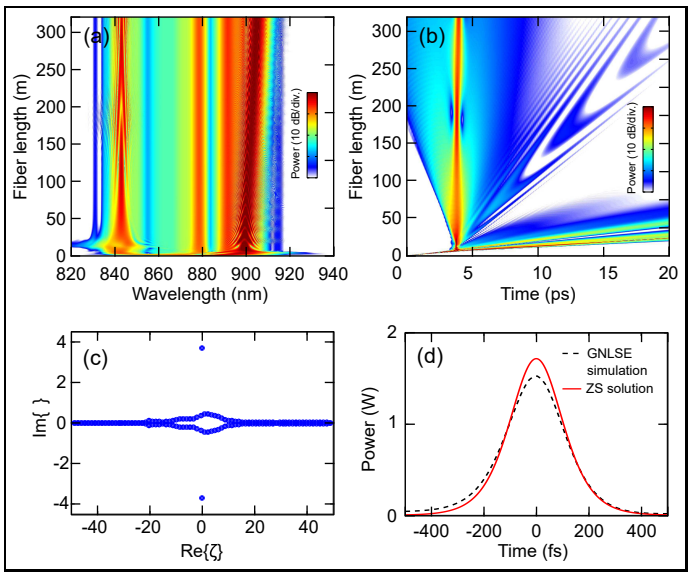


**Fig. 2.** (a) Spectral and (b) temporal dynamics for a fiber length of 320 m. (c) ZS spectrum calculated at 17 m. (d) Temporal profile of the 840 nm pulse obtained from GNLSE simulations at 320 m (black dashed line) and from the discrete eigenvalue of the ZS scattering problem (red solid line).

ration, with a central wavelength of 881 nm and a peak power of 42 W. The ZDW of the fiber is 875 nm which is close enough to the soliton central wavelength so that its spectrum overlaps with the normal dispersion region and therefore a dispersive wave is emitted around 840 nm, as can be observed in Fig. 1(b). In the time domain plot of Fig. 1(d), it appears at the trailing edge of the soliton, around 1 ps. After 4.9 m of propagation, the fiber dispersion $\beta_2$ is rapidly changed so that it becomes anomalous at the dispersive wave wavelength. More precisely, it goes from $5.4 \times 10^{-27}$ s$^2$/m to $-1.7 \times 10^{-27}$ s$^2$/m at 842 nm, and the ZDW is decreased from 875 nm to 832 nm. It is then kept constant until the fiber end. No significant change is observed in the spectral domain, but the time domain map of Fig. 1(d) shows that this dispersion sign change significantly modifies the trajectory of the dispersive wave. Indeed, while it was decelerating and starting to spread out in time until 5 m, it becomes accelerated in the tapered region, passes through the soliton and finally becomes compressed along propagation. There is no significant interaction between the soliton and the dispersive wave as the point where they overlap in time, because their group-velocity mismatch is too important [18]. The simulated temporal trace at the fiber output is displayed in Fig. 1(c). It shows that the dispersive wave (located around $-5$ ps) is indeed compressed to a short pulse with a clean temporal profile and a peak power of 6 W, comparable to that of the soliton located around 5 ps (of 14 W). The corresponding spectral peak is located around 840 nm (at the wavelength of the initial dispersive wave) in the output spectrum of Fig. 1(a).

In order to clarify the nonlinear nature of this pulse more precisely, we studied numerically its long term evolution in order to check whether it is able to propagate without significant deformation (as a soliton) or not. Figures 2(a) and (b) show respectively the spectral and temporal evolutions corresponding to the 17 m-long section displayed in Fig. 1(b), in a fiber with a longer uniform section similar to that of the taper end. We choose here a time reference co-moving with the solitonized dispersive wave. These figures show that the solitonized dispersive wave located at 840 nm indeed behaves like a soliton, as its spectral and temporal properties almost do not evolve over hundreds of meters. Figure 2(b) shows that the solitonized dispersive wave continuously emits small radiations along propagation. It also exhibits a slight, quasi periodic, temporal compression (only one period is shown in the figure). This is due to the fact that the pulse formed at the output of the tapered section is not a perfect fundamental soliton (we estimated $N = 1.6$ here) and as a consequence, it continuously adapts its shape to tend as closely as possible to the $N = 1$ condition. To show rigorously the validity of our interpretation, we analyzed the shape of the solitonized dispersive wave along propagation by numerically solving the Zakharov-Shabat direct scattering problem [19], with the Fourier collocation method [20]. In doing this, we neglect for the moment the Raman and higher-order dispersive effects and we take a constant value of the second-order dispersion, evaluated at 842 nm. In this way, the GNLSE reduces to the integrable case, to which the Inverse Scattering Transform (IST) applies. Before calculating the ZS spectrum, we filtered wavelengths higher than 860 nm, because we are interested exclusively to the ZS spectrum of the solitonized dispersive wave, and not of the whole field. Moreover we multiply the profile to be analyzed by $\exp[i\Delta\omega t]$, where $\Delta\omega$ is the frequency detuning between the field to be analyzed centered around 842 nm and the reference frequency of the GNLSE that is 881 nm. It is convenient to write the integrable nonlinear Schrödinger equation (NLSE) in the following normalized form:

$$i\partial_Z u + \partial_{TT} u + 2|u|^2 u = 0, \qquad (2)$$

where $T = t/t_0$, $Z = z|\beta_2|/(2t_0^2)$, $u = At_0\sqrt{\gamma/|\beta_2|}$, and $t_0$ is a

reference time (for instance 1 ps). The IST method is based on the possibility to write NLSE as the compatibility condition of two linear equations $Y_T = L(u,\zeta)Y$ and $Y_Z = M(u,\zeta)Y$, where $\zeta$ is a spectral parameter, and $Y(T,Z,\zeta)$ is vector function. The temporal equation

$$Y_T = \begin{bmatrix} -i\zeta & u \\ -u^* & i\zeta \end{bmatrix} Y, \quad (3)$$

is the ZS scattering problem. The discrete spectrum of the ZS operator is associated with solitons, whereas the continuous spectrum gives linearly dispersing waves (radiation). Indeed the soliton solution of normalized NLSE can be written as $u(T,0) = 2\eta\,\mathrm{sech}(2\eta T)\exp[-2i\xi T]$, where $\zeta = \xi + i\eta$. The soliton peak amplitude $2\eta$, and its velocity $-4\xi$ can be directly related to the ZS eigenvalue. From this analysis, we have found that the pulse centered around 840 nm indeed contains one fundamental soliton, corresponding to the discrete eigenvalue of the ZS problem. The ZS spectrum calculated at $z = 17$ m is reported in Fig. 2(c). We clearly see the discrete eigenvalue $\zeta = 3.7$, corresponding to one fundamental soliton propagating with zero velocity [in the reference frame of Eq. (2)]. The red curve in Fig. 2(d) compares the soliton shape obtained at 17 m from this analysis with the one simulated using the GNLSE (black line) at 320 m, corresponding to the output pulse of Fig. 2(b). Both pulse shapes match very well in terms of duration and peak power, thus proving that the dispersive wave has indeed been transformed into a fundamental soliton. This is confirmed by the value of the time-bandwith product (TBP) estimated from GNLSE simulations, which is equal to 0.33 at the end of the propagation.

Having demonstrated numerically the solitonization process, our next step was to attempt an experimental demonstration. For that, the PCF designed for the simulations of Fig. 1 has been fabricated. It has the same properties as detailed in the text describing Fig. 1. The pump parameters are identical to the ones of numerical simulations (Gaussian Fourier transform limited pulses of 140 fs FWHM duration centered around 881 nm). Figure 3(a) shows the spectral evolution versus fiber length for the initial 17 m-long axially-varying PCF. It was obtained by measuring the output spectrum after successive cutbacks performed every 1 m. The overall evolution is in excellent agreement with the simulations of Fig. 1(b). As discussed above, the spectral evolution does not provide any significant information about the solitonization process, which is why we also performed time domain measurements during the cutback experiment. To do that, the radiation located at 840 nm was spectrally filtered using a short-pass filter with a cutoff wavelength of 850 nm, and its non-collinear autocorrelation trace was measured. Figure 3(b) shows the evolution of the pulse duration with fiber length deduced from autocorrelation measurements (full circles) and the pulse duration obtained from numerical simulations (solid line). The measured autocorrelation traces are well fitted by a squared hyperbolic secant function, except for the first four points located before and within the tapered section for which the temporal profile of the dispersive wave was distorted. The FWHM durations are deducted using the deconvolution factor (equal to 0.65). For the first four points however, this roughly corresponds to the duration of the overall pulse envelope, as the finest details [as seen in the inset of Fig. 2(c)] could not be resolved. Despite that, experimental pulse durations are found to be in a good agreement and follow the same evolution as the numerical results. Figures 3(c) and (d)

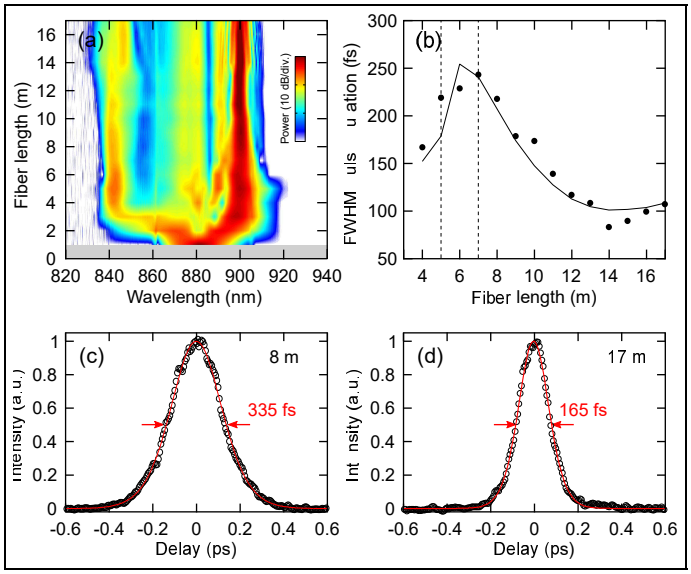


**Fig. 3.** (a) Spectral dynamics measured using successive cutbacks. (b) FWHM duration of the 840 nm pulse deduced from autocorrelation measurements using an hyperbolic secant function (full circles) and simulated FWHM duration using the GNLSE (solid line). Black dashed lines depict the start and end of the tapered section. (c)-(d) Measured autocorrelation traces (open circles) and squared hyperbolic secant fits (red solid lines) at (c) 8 m (after the tapered region) and (d) 17 m (fiber output).

show two examples of measured autocorrelation traces (open circles) at 7 m and 17 m respectively, with their squared hyperbolic secant fit (red solid lines). The measurements and the fits agree well, especially at the PCF output (17 m) where the soliton has had the time to form. Remarkably, the dispersive wave, whose duration almost reaches 250 fs at 7 m, is compressed to a 100 fs pulse during the solitonization process occurring within the tapered section. By comparison, its duration would reach 1.5 ps at the output of a 17 m-long uniform in fiber (*i.e.* with no tapering section).

To summarize, we have shown numerically and experimentally that a dispersive wave emitted from a soliton can be itself transformed into a fundamental soliton by carefully varying the longitudinal evolution of dispersion. The solitonic nature of the resulting pulse has been demonstrated by solving the direct Zakharov-Shabat scattering problem, which gives excellent agreement with simulations and experiments. This process is opposite to the one recently observed in [21] in which a fundamental soliton becomes annihilated into a polychromatic dispersive wave thanks to the axially-varying dispersion.

From an applicative point of view, the results reported here show the possibility of delivering two fundamental solitons of different wavelengths with comparable peak power, as seen in Fig. 1(c). The wavelength separation between the two solitons can be adjusted by modifying the fiber design and their relative delay (in the order of picoseconds) can easily be compensated with an optical delay line. These properties would make the whole system a promising solution for the development of two-color ultrashort pulse source, usable for pump-probe experiments for instance.

## FUNDING INFORMATION

This work was partly supported by the ANR TOPWAVE (ANR-13-JS04-0004) and NoAWE (ANR-14-ACHN-0014) projects, by the "Fonds Européen de Développement Economique Régional", the Labex CEMPI (ANR-11-LABX-0007) and Equipex FLUX (ANR-11-EQPX-0017) through the "Programme Investissements d'Avenir".

## REFERENCES

1. L. F. Mollenauer, R. H. Stolen, and J. P. Gordon, Phys. Rev. Lett. **45**, 1095 (1980).
2. J. R. Taylor, *Optical Solitons: Theory and Experiment* (Cambridge University Press, 2005).
3. L. F. Mollenauer and K. Smith, Opt. Lett. **13**, 675 (1988).
4. E. R. Andresen and H. Rigneault, Opt. Fiber Technol. **18**, 379(2012).
5. C. Xu and F. W. Wise, Nat. Photon. **7**, 875 (2013).
6. S. Saint-Jalm, E. R. Andresen, P. Ferrand, A. Bendahmane, A. Mussot, O. Vanvincq, G. Bouwmans, A. Kudlinski, and H. Rigneault, J. Biomed. Opt. **19**, 086021 (2014).
7. G. Agrawal, *Nonlinear Fiber Optics, Fifth Edition* (Academic Press, Amsterdam, 2012), 5th ed.
8. P. Beaud, W. Hodel, B. Zysset, and H. Weber, IEEE J. of Quantum Elect. **23**, 1938 (1987).
9. J. K. Lucek and K. J. Blow, Phys. Rev. A **45**, 6666 (1992).
10. R. Driben, B. A. Malomed, A. V. Yulin, and D. V. Skryabin, Phys. Rev. A **87**, 063808 (2013).
11. P. K. A. Wai, C. R. Menyuk, Y. C. Lee, and H. H. Chen, Opt. Lett. **11**, 464 (1986).
12. P. K. A. Wai, C. R. Menyuk, H. H. Chen, and Y. C. Lee, Opt. Lett. **12**, 628 (1987).
13. N. Akhmediev and M. Karlsson, Phys. Rev. A **51**, 2602 (1995).
14. A. Bendahmane, F. Braud, M. Conforti, B. Barviau, A. Mussot, and A. Kudlinski, Optica **1**, 243 (2014).
15. C. Conti, Phys. Rev. A **86**, 061801 (2012).
16. D. Hollenbeck and C. D. Cantrell, J. Opt. Soc. Am. B **19**, 2886 (2002).
17. K. Saitoh and M. Koshiba, Opt. Express **13**, 267 (2005).
18. S. F. Wang, A. Mussot, M. Conforti, A. Bendahmane, X. L. Zeng, and A. Kudlinski, Phys. Rev. A **92**, 023837 (2015).
19. V. E. Zakharov and A. B. Shabat, Sov. Phys. JETP **34**, 62 (1972).
20. J. Yang, *Nonlinear Waves in Integrable and Nonintegrable Systems* (SIAM, Philadelphia, 2012), 1st ed.
21. A. Kudlinski, S. F. Wang, A. Mussot, and M. Conforti, Opt. Lett. **40**, 2142 (2015).

## INFORMATIONAL FIFTH PAGE

## REFERENCES


1. L. F. Mollenauer, R. H. Stolen, and J. P. Gordon, “Experimental observation of picosecond pulse narrowing and solitons in optical fibers,” Phys. Rev. Lett. **45**, 1095–1098 (1980).
2. J. R. Taylor, *Optical Solitons: Theory and Experiment* (Cambridge University Press, 2005).
3. L. F. Mollenauer and K. Smith, “Demonstration of soliton transmission over more than 4000 km in fiber with loss periodically compensated by Raman gain,” Opt. Lett. **13**, 675–677 (1988).
4. E. R. Andresen and H. Rigneault, “Soliton dynamics in photonic-crystal fibers for coherent Raman microspectroscopy and microscopy,” Opt. Fiber Technol. **18**, 379–387 (2012).
5. C. Xu and F. W. Wise, “Recent advances in fibre lasers for nonlinear microscopy,” Nat. Photon. **7**, 875–882 (2013).
6. S. Saint-Jalm, E. R. Andresen, P. Ferrand, A. Bendahmane, A. Mussot, O. Vanvincq, G. Bouwmans, A. Kudlinski, and H. Rigneault, "Fiber based ultra-short pulse delivery for nonlinear imaging using high energy solitons," J. Biomed. Opt. **19**, 086021 (2014).
7. G. Agrawal, *Nonlinear Fiber Optics, Fifth Edition* (Academic Press, Amsterdam, 2012), 5th ed.
8. P. Beaud, W. Hodel, B. Zysset, and H. Weber, “Ultrashort pulse propagation, pulse breakup, and fundamental soliton formation in a single-mode optical fiber,” IEEE J. of Quantum Elect. **23**, 1938–1946 (1987).
9. J. K. Lucek and K. J. Blow, “Soliton self-frequency shift in telecommunications fiber,” Phys. Rev. A **45**, 6666–6674 (1992).
10. R. Driben, B. A. Malomed, A. V. Yulin, and D. V. Skryabin, “Newton’s cradles in optics: From $N$-soliton fission to soliton chains,” Phys. Rev. A **87**, 063808 (2013).
11. P. K. A. Wai, C. R. Menyuk, Y. C. Lee, and H. H. Chen, “Nonlinear pulse propagation in the neighborhood of the zero-dispersion wavelength of monomode optical fibers,” Opt. Lett. **11**, 464–466 (1986).
12. P. K. A. Wai, C. R. Menyuk, H. H. Chen, and Y. C. Lee, “Soliton at the zero-group-dispersion wavelength of a single-model fiber,” Opt. Lett. **12**, 628–630 (1987).
13. N. Akhmediev and M. Karlsson, “Cherenkov radiation emitted by solitons in optical fibers,” Phys. Rev. A **51**, 2602–2607 (1995).
14. A. Bendahmane, F. Braud, M. Conforti, B. Barviau, A. Mussot, and A. Kudlinski, “Dynamics of cascaded resonant radiations in a dispersion-varying optical fiber,” Optica **1**, 243–249 (2014).
15. C. Conti, “Solitonization of the Anderson localization,” Phys. Rev. A **86**, 061801 (2012).
16. D. Hollenbeck and C. D. Cantrell, “Multiple-vibrational-mode model for fiber-optic Raman gain spectrum and response function,” J. Opt. Soc. Am. B **19**, 2886–2892 (2002).
17. K. Saitoh and M. Koshiba, “Empirical relations for simple design of photonic crystal fibers,” Opt. Express **13**, 267–274 (2005).
18. S. F. Wang, A. Mussot, M. Conforti, A. Bendahmane, X. L. Zeng, and A. Kudlinski, "Optical event horizons from the collision of a soliton and its own dispersive wave," Phys. Rev. A **92**, 023837 (2015).
19. V. E. Zakharov and A. B. Shabat, “Exact theory of two-dimensional self-focusing and onedimensional self-modulation of waves in nonlinear media,” Sov. Phys. JETP **34**, 62–69 (1972).
20. J. Yang, *Nonlinear Waves in Integrable and Nonintegrable Systems* (SIAM, Philadelphia, 2012), 1st ed.
21. A. Kudlinski, S. F. Wang, A. Mussot, and M. Conforti, "Soliton annihilation into a polychromatic dispersive wave," Opt. Lett. **40**, 2142–2145 (2015).